



**HAL**  
open science

## Finite element analysis of the Meuse Haute-Marne underground research laboratory

Farid Laouafa, Gilles Armand, Jean-Bernard Kazmierczak, Tatiana Maison

### ► To cite this version:

Farid Laouafa, Gilles Armand, Jean-Bernard Kazmierczak, Tatiana Maison. Finite element analysis of the Meuse Haute-Marne underground research laboratory. 1. International Symposium on computational geomechanics (COMGEO 2009), Apr 2009, Juan-les-Pins, France. pp.680-690. ineris-00973340

**HAL Id: ineris-00973340**

**<https://ineris.hal.science/ineris-00973340>**

Submitted on 4 Apr 2014

**HAL** is a multi-disciplinary open access archive for the deposit and dissemination of scientific research documents, whether they are published or not. The documents may come from teaching and research institutions in France or abroad, or from public or private research centers.

L'archive ouverte pluridisciplinaire **HAL**, est destinée au dépôt et à la diffusion de documents scientifiques de niveau recherche, publiés ou non, émanant des établissements d'enseignement et de recherche français ou étrangers, des laboratoires publics ou privés.

# FINITE ELEMENT ANALYSIS OF THE MEUSE HAUTE-MARNE UNDERGROUND RESEARCH LABORATORY

F. Laouafa

*INERIS - Parc technologique ALATA, BP 2, 60550 Verneuil-en-Halatte, France*

G. Armand

*ANDRA- Laboratoire de recherche souterrain de Meuse Haute Marne, Route départementale 960, 55290 Bure, France*

J.B. Kazmierczak

*INERIS - Parc technologique ALATA, BP 2, 60550 Verneuil-en-Halatte, France*

T. Maison

*Laboratoire MSSMat, UMR CNRS 8579, Ecole Centrale Paris, Grande Voie des Vignes, 92295 Châtenay-Malabry cedex & INERIS*

**ABSTRACT:** *The Meuse/Haute-Marne Underground Research Laboratory (ANDRA) has been excavated to study the feasibility of a deep underground repository in the Callovo-Oxfordian argillite. The laboratory, lying at depth between 420 m and 550 m, has a complex structure due to the shape and location of various shafts and drifts. The purpose of this study is to analyse the mechanical behaviour of rock due to the excavation process, and the mechanical interaction between drifts and shafts during the excavation steps. Numerical analysis, which considers the geometry and excavation sequence of the Underground Research Laboratory (URL), is carried out using a finite element model having 2.5 million degrees of freedom with relatively simple constitutive equations describing the argillite's behaviour. The main interest of such large-scale modelling is to analyse the evolution of various mechanical fields during excavation progress. Indeed, comparisons between 2D and 3D analysis are performed and show that the 2D-plane strains assumption is no longer fulfilled in some areas of the laboratory. The results of the analysis are used to highlight areas where interaction between drifts and/or shafts is important. It is helpful to restrict the field of the analyses using some relevant criterion or appropriate boundary conditions, to perform the numerical simulations based on a more realistic elasto-visco-plastic constitutive model for rocks.*

## 1 INTRODUCTION

The Meuse/Haute-Marne Underground Research Laboratory (URL) is located on the eastern boundary of the Paris basin, at the border of the Champagne-Ardenne and Lorraine regions, at Bure. The French national radioactive waste management agency (Andra) (Andra 2005a,b) started to build this URL in the year 2000 in order to demonstrate the feasibility of a radioactive waste repository in claystone formation (Piguet, 2001). The host formation consists of claystone (Callovo-Oxfordian argillaceous stone) layer, 130 m thick lying at a depth of approximately 500 meters (middle of the layer) (Andra 2005). The Callovo-Oxfordian clays are overlain and underlain by poorly permeable carbonate formations. The objectives of the URL during the 2000 -2006 period were mainly *in-situ* characterization of the physical and chemical properties of this rock. This involved achieving a level of knowledge that may be used to develop disposal designs and perform safety studies. The confining properties of the clay were studied through *in-situ* hydrogeological experiments, chemical measurements and diffusion analyses. An understanding of the fundamental physical and chemical properties and processes that govern geological isolation in clay-rich

rocks has been acquired (Delay et al 2007a). This knowledge includes both the host rocks at the laboratory site and the regional geological context.

Another aspect of the research program was to demonstrate that the construction and operation of a geological disposal will not create pathways which allow radionuclide migration. This study involved a deep understanding of the hydro-mechanical behavior and of building impacts (the excavation-damaged zone, for instance). That is why the construction of the laboratory itself serves a research purpose by way of in situ monitoring of the excavation effects and for the optimization of construction technology.

The underground components of the laboratory consist of two shafts and several drifts constructed for scientific and technical purposes. As the in situ stress field is anisotropic, the drift network has been excavated in order to investigate hydromechanical drift behavior in the direction of both principal stresses. This means that, in order to meet the geomechanical issues, experiments are performed in drift parallel and/or perpendicular to the major horizontal stress. The whole of the laboratory is mainly located in a volume of several million cubic meters in the Callovo-Oxfordian layer.

Several numerical modeling has already been done in order to predict and analyze the *in-situ* measurements, mainly the time evolution of strains and pore pressures. However, most of the numerical models usually focused on the specific area where instrumented boreholes have been located. The following two questions could be asked: Is it relevant or necessary to understand the effect of this drift network on stress distribution and accurately evaluate the stress state at the URL main level? And secondly: during a stage-by-stage construction of the different drifts, can we measure the mechanical interaction between drifts and their intensity? Andra started a new research program which requires an expanse of the URL drifts. New drifts will be excavated for new scientific analyses (Delay *et al*, 2007b). What effect will these new excavations have on the existing drifts? On the other hand, is it possible to situate experiments in areas where we are sure that the stress field has not been disturbed by the previous excavation works? Nowadays computers with larger memory and faster processors, make it feasible to study larger computational models.

This paper presents, in the first part, some modeling results of a 3D study performed to analyze the mechanical behavior of all of the drifts in the Callovo-Oxfordien layer by using a chronological evolution (time stepping) of the excavations, close to what was realized in reality. In the second part, we performed a comparison of some fields arising from the 3D computations to those resulting from a 2D plane strain assumption. These comparisons are performed for several vertical planes of the URL. We clearly show that the 2D assumption is no longer valid. Let us emphasize that this comparison is performed in a purely mechanical framework (no thermal or hydraulic coupling).

The 3D elastic or elastoplastic modeling is, in our opinion, interesting, because as it is commonly performed in monitored in situ field, the numerical results provide information on the more disrupted area and one can then conduct a more accurate analysis, involving more realistic physical laws, in restricted areas which noticeably reduce computation times.

Considering the size and the complex geometry of the problem, the analyses are carried out by finite elements with relatively simple constitutive models describing the argillites' mechanical behavior. Finally, we discuss the scientific contribution of such huge computations and provide some recommendations for future work.

## **2 GENERAL DESIGN**

The underground installations consist of two shafts and drift networks (Delay et al (2007 b)). The main shaft, 5 meters in diameter after lining, grants access to a 445 meter deep drift

network and to the 490 meter deep main drift network. The auxiliary shaft, 4 meters in diameter after lining, is also connected to the URL's main level.

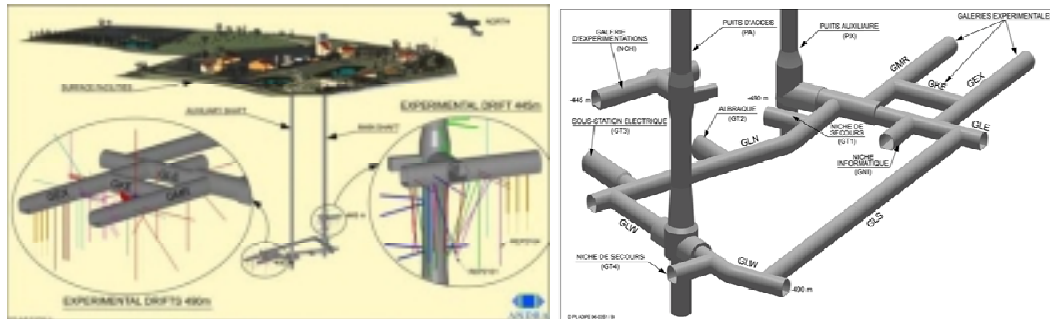


Fig. 1. General view of the Meuse Haute Mame Underground research laboratory (mid to late 2006)

Drifts have a “horse shoe” cross section. The drift network at 445 m is 45-meter long and T-shaped. This experimental zone has been equipped to perform monitoring of a mine by testing during shaft sinking. These drifts are 17 m<sup>2</sup> in section. At the main level located at 490 m, the network consists of experimental and technical drifts. By mid 2007, this network was 485 meter-long, out of which 80 meters are dedicated to experiments. The orientation of the scientific drifts has been determined according to the orientation of in situ stress fields (Wileveau et al., 2007a). The current section of the drifts is 17 m<sup>2</sup>; however, some technical zones have been excavated in different diameters, up to 40 m<sup>2</sup>.

Drift excavation methods depended on the nature of the rock mass they passed through. A drill-and-blast technique was used to excavate the 445 meter-deep drift. Rock bolts were set in place after blasting. Support consists of rock bolts and sliding arches. A concrete raft was installed to facilitate displacements.

At the main level, a stone crushing technique was used for excavation. Bolts and sliding arches were set in place immediately following a two-meter maximum progression. At minimum, a 10 cm-thick layer of concrete was applied on all of the drift walls to limit the spalling induced by drift convergence.

Construction of the underground installations started in August 2000 with the sinking of the main shaft and was completed on 27 April 2006, when it linked up with the southern drift of the laboratory. Equipment of the laboratory was completed in July 2007 with the installation of the hydraulic and electrical networks. This sums up the main stages of the laboratory construction.

The geometrical model takes the drift and shafts in the Callovo-Oxfordien layer into account. In order to take the excavation evolution versus time into account, the numerical excavation was performed in 26 steps based on monthly excavation rates actually performed *in situ*. In the experimental area, formed by GLE, GKE, GMR and GEX drifts (Fig. 1), the time stepping was reduced to weeks to better analyze interference between those drifts in the area where sensors have been placed.

Scientific actions were carried out concurrently with the sinking and excavating. They consisted of a systematic geological mapping, closure measurements and drilling of boreholes to measure pore pressure and displacement (Delay *et al*, 2007b).

### 3 3D FINITE ELEMENT COMPUTATIONS

#### 3.1 Assumptions

The main difficulties of the 3D and time stepping analysis lie in the construction of the complex geometry of the network of galleries and the associated mesh. The entirety of the galleries and wells of the URL is shown at the level of the Callovo-Oxfordien (Fig. 2). One of the main difficulties of this 3D and time stepping analysis lies in the construction of the geometry of the network of galleries and the associated mesh. The geometric shape of the different galleries, the wells, as well as their arrangement and their intersection generates an extremely complex geometry. The entirety of the galleries and wells of the URL is shown at the level of the Callovo-Oxfordien (Fig. 2). The exact geometry is defined in the section above.

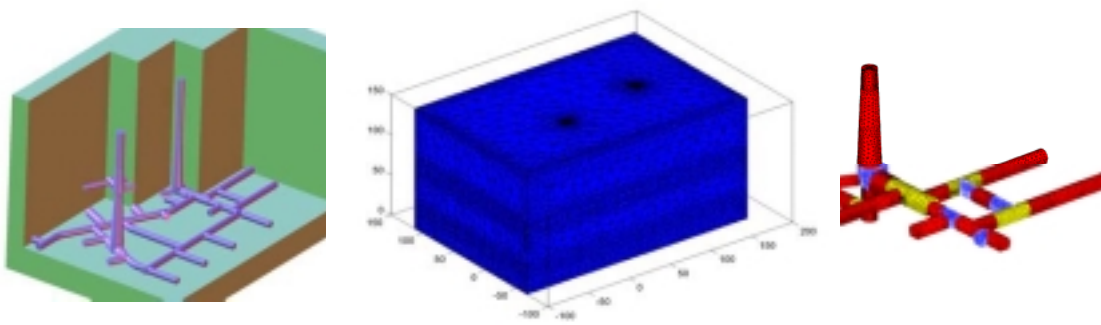


Fig. 2. From left to right: part of geometrical model, mesh of the domain and detail of gallery and wells

The computations were performed with COMSOL MULTIPHYSICS finite element code (Comsol, 2006). The domain used in our modeling has the following dimensions: the length (in the  $x$  direction) is equal to  $270\text{ m}$ , the width (in the  $y$  direction) is equal to  $180\text{ m}$  and finally the height (in the  $z$  direction) is equal to  $150\text{ m}$ . The frame of reference ( $O,x,y,z$ ) is shown on the right of Figure 3. Such a dimension leads to an analysis volume equal to  $7.290.000\text{ m}^3$ . The upper level of the model corresponds to a depth of 398 meters. The domain is defined as follows:

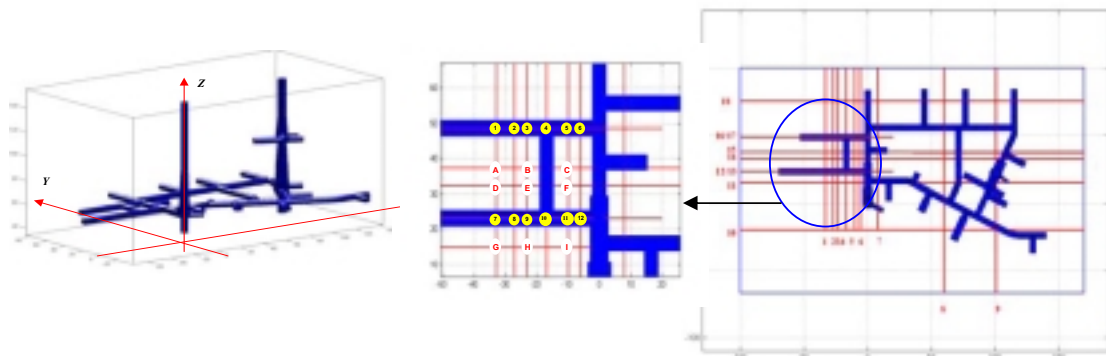


Fig. 3. Reference frame (left) and lines (planes) and points of analysis (right)

The finite element mesh is made up of 603,325 quadratic tetrahedrons, which leads to a number of degree of freedom equal to 2,452,635. The kinematical boundary conditions are imposed on all vertical boundaries and on the bottom of the model as follows:  $\underline{U} \cdot \underline{n} = 0$ . This

defines five planes of symmetry ( $n$  is the outward unit normal to these boundaries). The only boundary tractions are applied on the top of the model and are equal to  $\underline{t}(x, y, z = 150 \text{ m}) = \underline{t} \equiv (t_x, t_y, t_z) = (0, 0, -9.95 \text{ MPa})$ , assuming a constant density  $\gamma$  of  $25 \text{ kN/m}^3$ . In terms of initial conditions, three assumptions are made: (i) the initial stress is principal in the reference frame:  $\sigma_{ij} = 0, \quad \forall i \neq j$ , (ii) at any point of the domain, the initial stress state is anisotropic and characterized by two coefficients  $K_{ox}$  and  $K_{oy}$  and (iii) at any point of the domain, the vertical stress  $\sigma_{zz}$  is equal to the weight of the overburden soil. Thus the initial anisotropic stress field is defined as follows:

$$\begin{cases} \sigma_{xx} = K_{ox} \times \sigma_{zz} \\ \sigma_{yy} = K_{oy} \times \sigma_{zz} \\ \sigma_{zz} = -9.95 - \gamma \times (150 - z) \end{cases} \quad \text{where} \quad K_{oy} = \frac{\sigma_{yy}(0)}{\sigma_{zz}(0)} = 1.3 \quad \text{and} \quad K_{ox} = \frac{\sigma_{xx}(0)}{\sigma_{zz}(0)} = 1 \quad (1)$$

### 3.2 Constitutive models

The analysis of the 3D study was performed by successively using two constitutive models. The first assumes linear isotropic elastic models for the different soil layers. The second analysis was performed using a simple elastic-perfectly plastic model. In this case we adopted a modified Drucker-Prager yield surface  $F(\underline{\sigma})$ . This yield surface passed through the inner vertex of the Mohr-Coulomb yield surface and is stated as follows (Lubliner, 1990):

$$F = \frac{2\sin(\phi)}{\sqrt{3}(3+\sin(\phi))} I_1 + \sqrt{J_2} - \frac{6C\sin(\phi)}{\sqrt{3}(3+\sin(\phi))} = 0 \quad (2)$$

where  $I_1$  is the first invariant of the stress tensor while  $J_2$  is the second invariant of the deviatoric stress tensor. The parameters  $C$  and  $\phi$  are the cohesion and the internal friction angle, respectively. Our geometric model contains three rocks layers. The different parameters are provided in the following tables 1 and 2.

Table 1. Elastic parameters for the three rock layers

Parameter	Value
Layer 1 – Young modulus $E_1$	5400 MPa
Layer 2 – Young modulus $E_2$	4500 MPa
Layer 3 – Young modulus $E_3$	4500 MPa
Poisson coefficient $\nu$	0.3

Table 2. Plastic parameters for the three rock layers

Parameter	Layer 1	Layer 2	Layer 3
Cohesion $C$ (MPa)	4	4	4
Cutting traction strength (MPa)	2.6	2.6	2.6
Friction angle ( $^\circ$ )	23	23	23

At this stage we may observe that for the purely elastic problems (linear problems), there was no risk of loss of ellipticity (Marsden, 1983) because the analysis is performed under the small strains hypothesis, and that the constitutive operator is positive definite in all material points of the domain. In light of the structures of the different networks of galleries, and of the "massive" structure of the model, all bifurcation problems, such as buckling or others, can be excluded (Hill, 1958, Rudnicki 1975). However, one can expect stress concentrations with very high intensity, and unrealistic, notably at the level of the corners and of some intersections. These singularities have no effect on the solution in the elastic computation because their influence decreased very quickly, as soon as one moves away from it. This is not the case for the nonlinear analysis, for which precautions are taken in the results analysis. Let us stress that in light of the number of degrees of freedom, we choose an iterative algorithm to resolve the linear or linearized problem. We utilized the preconditioned GMRES algorithm (Saad, 1986) that showed itself to be more robust than the preconditioned conjugate gradient. As soon as the initial and boundary conditions were assigned, 26 excavation steps were performed inside the different layers, where each one corresponds roughly to a monthly excavation step.

### 3.3 3D numerical results

Figures 4, 5 and 6 depict the disrupted area in terms of displacement.

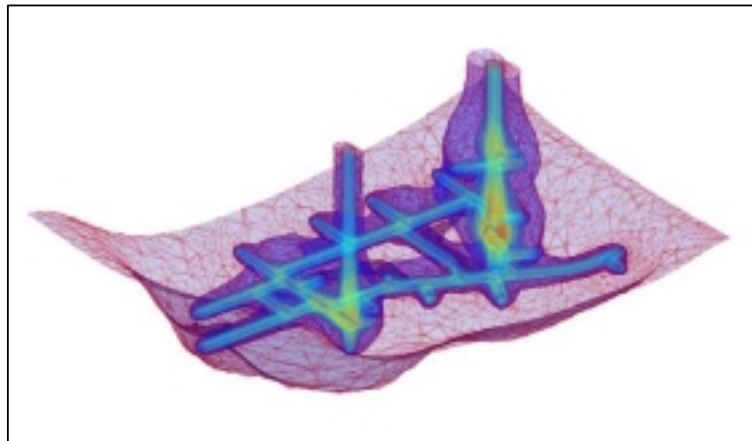


Fig. 4. 3D view of the disrupted area in terms of displacement at the end of excavation process

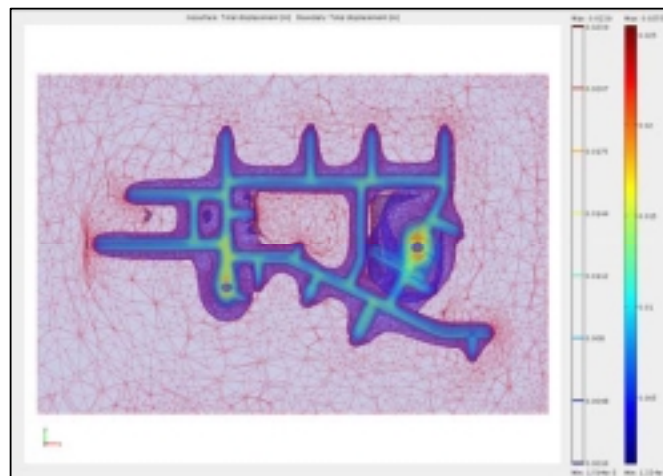


Fig. 5. Top view of the disrupted area in terms of displacement at the end of excavation process

As we can see, the disrupted zone remains close to drifts and wells. The greater displacements (amplitude varying from 5 mm to 4 cm) are measured on the boundaries of the galleries.

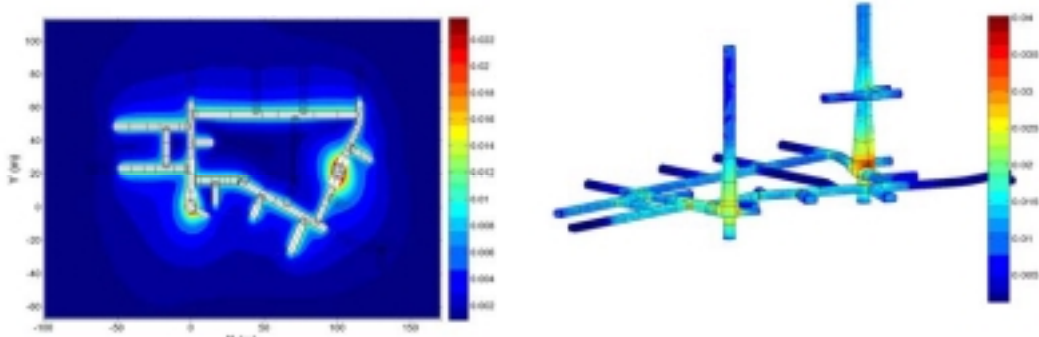


Fig. 6. Example of isovalues of the Euclidean displacement norm in the horizontal plane passing through the middle of the laboratory on the left. Isovalues of the Euclidean displacement norm in the boundaries of the different shafts and drifts.

In Figure 7, we show an example of the time (excavation step) evolution of stress and displacement components of point A (Fig. 3).

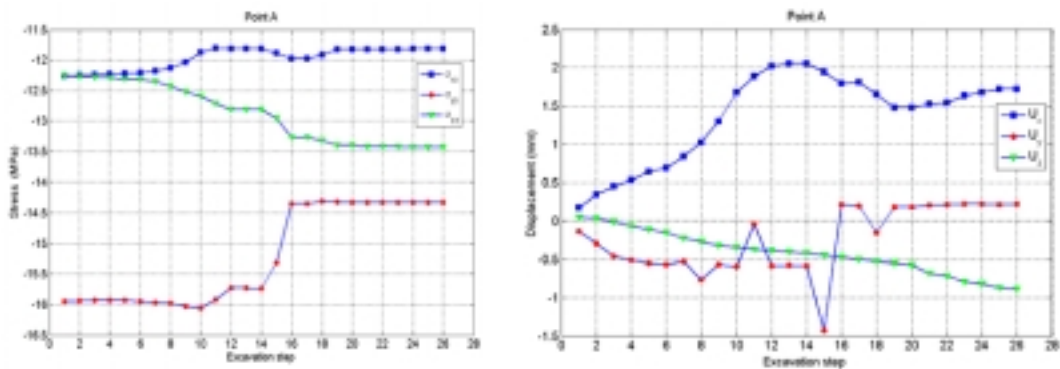


Fig. 7. Example of evolution of stress and displacement components during excavation process

It is interesting to note that no component remains constant and that the stress and displacement norms at the (y-z) plane (plane for plane strain analysis) evolve non-uniformly. This point will be discussed in the next section. In Figure 8 we show, on the left, the monitoring of relative vertical displacement between the drift located at a depth equal to 447 meters and five points distributed vertically above in the soil within the limit of 20 meters.

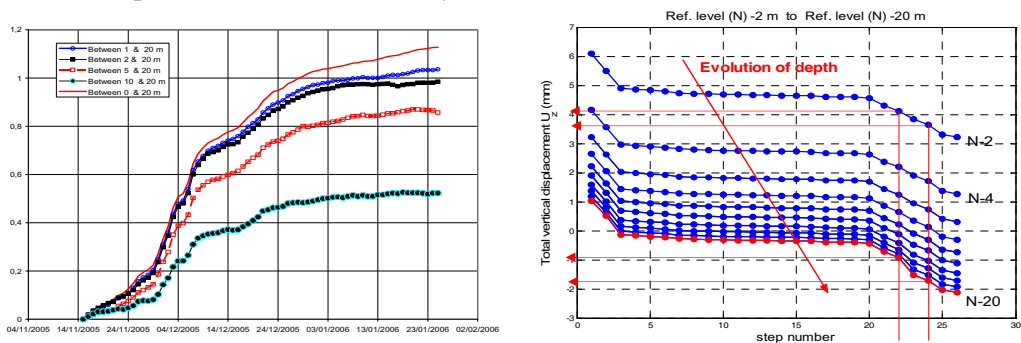


Fig. 8. Relative displacement monitoring in situ (left) during two months and computational total displacement for the 26 steps.

The measured relative displacement is from 0.51 *mm* to 1.05 *mm*. The computational relative displacement obtained from the graph of Figure 12 (right) gives a relative displacement from 0.5 *mm* to 1 *mm*, thus in very good agreement with the measured variable. Just note that this agreement is observed far away from the drift in an area where the rock behavior is nearly elastic. In the vicinity of the drift, those calculations cannot provide an accurate estimate of relative displacement. At the main level of the URL, geological mapping of the front faces and structural analysis on the drill core exhibit a fracture pattern around the drift *showing the occurrence of non-elastic deformations*.

#### 4 3D VS. PLANE STRAIN FINITE ELEMENT COMPUTATIONS

The figure below indicates the different planes of the 2D analyses. Five planes passing through lines 1, 2, 3, 4 and 6 are considered.

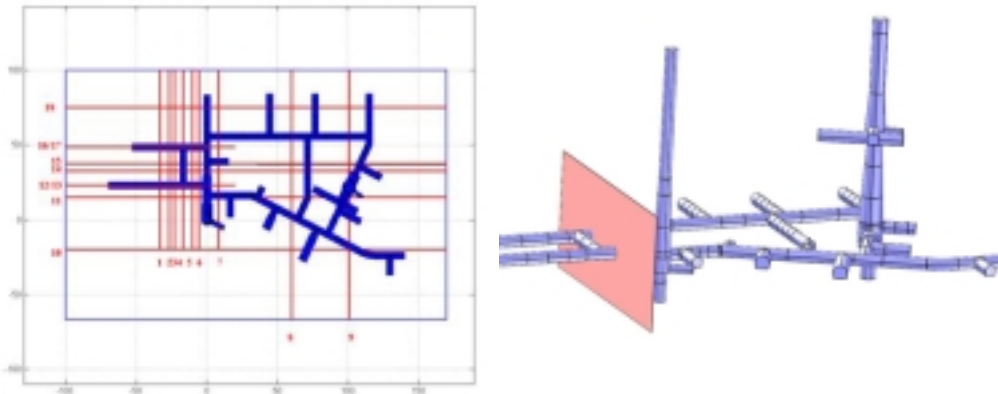


Fig. 9. Spatial location of the plane used in plane strains analyses

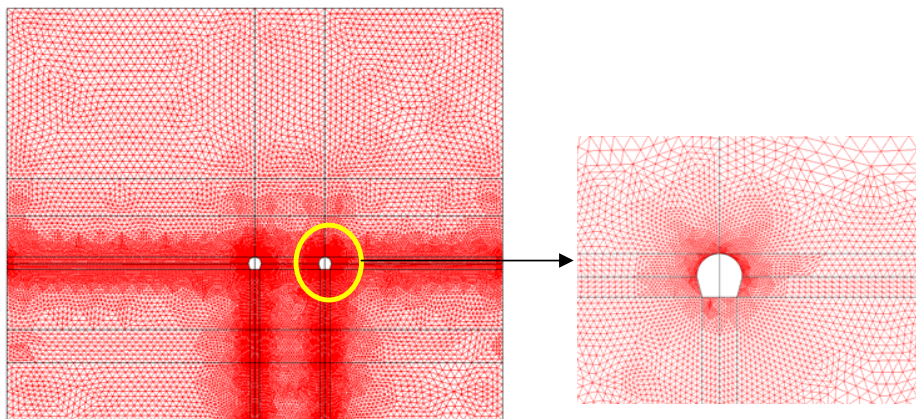


Fig. 10. Finite element mesh used in plane strains analyses

Figures 9 and 10 provide information about the 5 locations of the different 2D planes and the mesh quality used in plane strain assumptions.

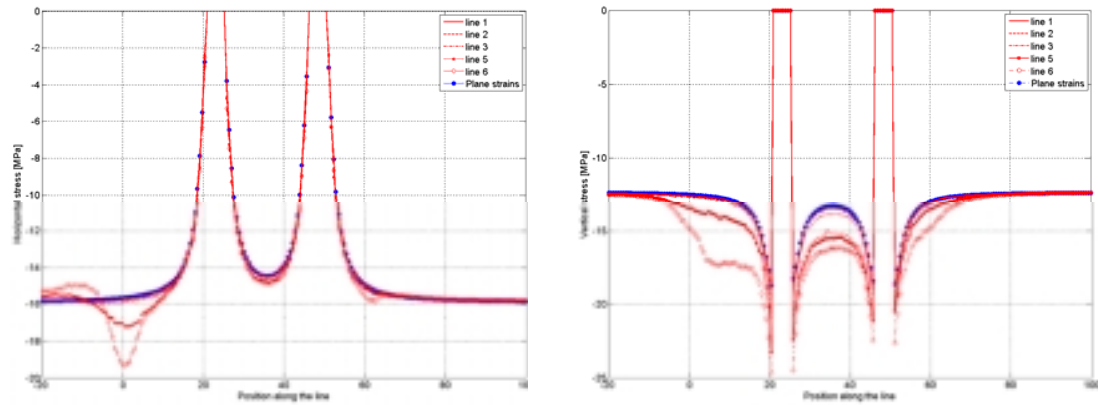


Fig. 11. 3D-2D comparison for two components of the stress tensor

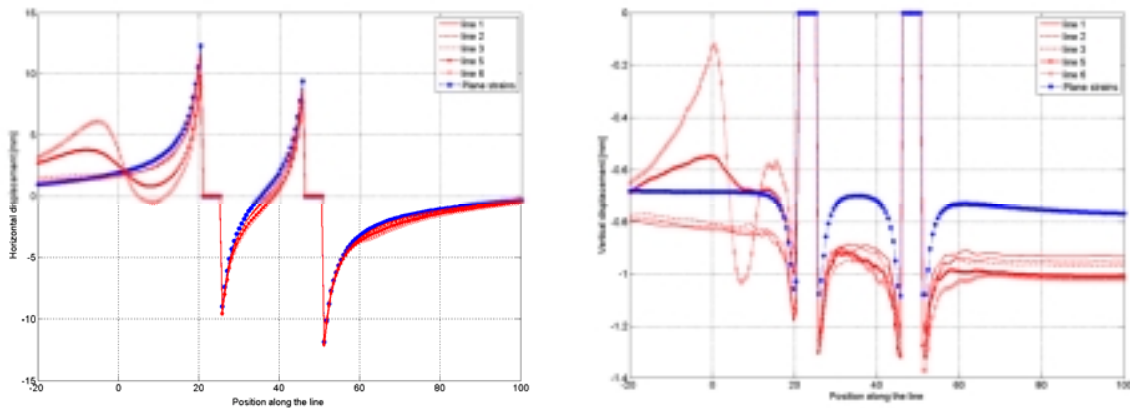


Fig. 12. 3D-2D comparison for two components of the displacement vector

We observe that the component of the stress tensor and displacement vector can be significantly different, which confirms that the plane strain assumption can be a strong hypothesis. Furthermore, we observe the mechanical influence of the shafts which disrupt the two mechanical fields. In Figure 9 we have depicted the location of different points and lines where a more accurate analysis was performed, in particular in term of stress, strain and displacement distribution and "time-excavation step" evolution.

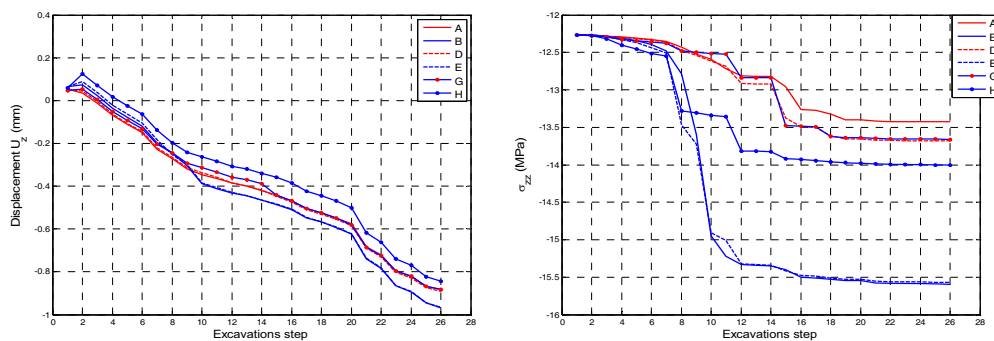


Fig.13: Evolution of vertical displacement (left) and vertical stress (right) at different material points.

While the evolution of vertical displacement for the different points seems smooth and quite similar, the evolution of the vertical stress clearly shows the influence or contribution of the two orthogonal excavations. Indeed, points B and E are the closest to the drift

intersection, and are both subjected to mechanical perturbations. The fact that this perturbation is less significant in the displacement field is linked to the fact that the stress or strain distribution is in  $O(r_0^2 / r^2)$  and then, the decreasing rate is of the order of 2, which means the stress or the stress perturbation decreases more quickly and affects a more restricted area.

Note that the same observations are made for the all of the points. The question of the usefulness of such purely mechanical 3D computations may be posed. Are plane strain or plane stress assumptions acceptable? The answer is clearly no, in some obvious zones, where the problem is locally really 3D. Elsewhere these assumptions could perhaps be accurate enough, in comparison with the many uncertainties.

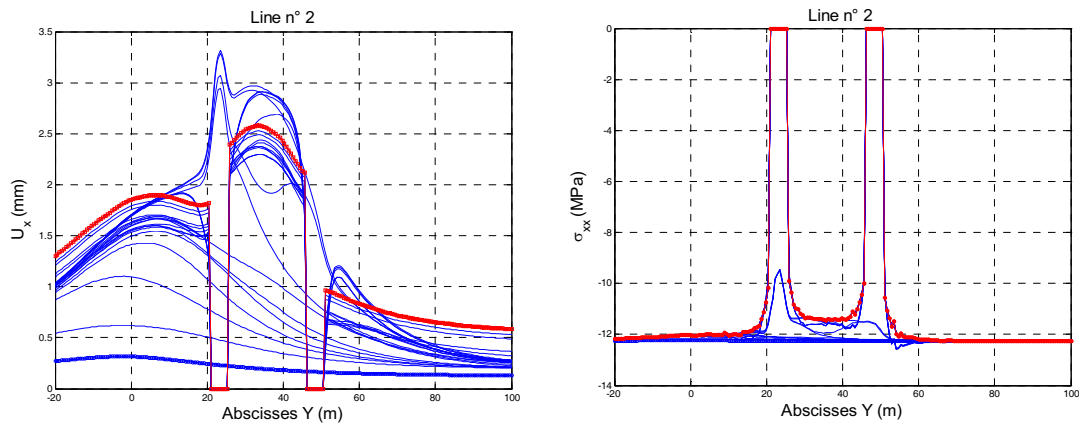


Fig 14. "Time" evolution and space distribution of horizontal  $U_x$  displacement (left) and horizontal stress  $\sigma_{xx}$  (right) for horizontal line n° 2 passing in the middle of the laboratory.

In order to answer to the question posed above, we analyze the results depicted in Figure 14. The red circles correspond to the last step, while the blue ones correspond to the first step of excavation. This line is chosen because it is far enough from its parallel drift and it is orthogonal to two excavated zones. In terms of  $U_x$ , we observe no constant distribution, except at the beginning of the excavation phase (the excavated zones are too far from this line). This graph demonstrates the "non-validity" of a plane strain assumption. The same remarks are made in terms of stress. We also observe no constant distribution, except at the beginning of the excavation phase (the excavated zones are too far from this line). This graph demonstrates the "non-validity" of a plane stress assumption. The sentence "non-validity" is between quotes to put our conclusion into context.

## 5 CONCLUDING REMARKS

We have briefly presented the 3D mechanical analysis of the Andra laboratory composed of several drifts and shafts and a comparison with computations based on a plane strain assumption. The mechanical behavior of such an underground structure has been investigated by the way of step-by-step, "huge" finite element computations. The aim of this work is to analyze the various mechanical interactions between the different components of the laboratory and to analyze their "time" evolution during the excavation. The relevance of such huge three-dimensional modeling is twofold.

The first aspect of this relevance is that the adopted approach provides several of information, namely on the spatial distribution and time evolution of the different mechanical fields (stress, strain and displacement).

Secondly, we have some measurements on the extension of perturbations induced by the different excavations, and the eventual interaction between the components of the laboratory. Such an analysis is difficult to circumvent, since the development of the laboratory evolves without any spatial or mechanical symmetry. This fact is demonstrated by several comparisons with purely mechanical 2D analyses. Although the constitutive models are relatively simple, such analysis provides interesting information and could be useful for a more accurate future analysis (coupling processes, creep model for instance). Let us underline that with such a simple model, the numerical results provide the correct trend observed in situ in terms of displacement.

## REFERENCES

- Andra, (2005a). Dossier 2005, synthesis, Evaluation of the feasibility of a geological disposal in an argillaceous formation, décembre 2005 (available at [www.andra.fr](http://www.andra.fr)).
- Andra, (2005b). – collectif, Dossier 2005 Argile - Référentiel du site Meuse/Haute-Marne. Andra report n° C.RP.ADS.04.0022, Andra, Ed. N°271 B à 275 B, December 2005.
- Delay, J., Vinsot, A., Krieguer, J.M., Rebours, H., Armand, G., (2007a). “Making of the underground scientific experimental programme at the Meuse/Haute-Marne underground research laboratory, North Eastern France”. *Physics and Chemistry of the Earth* 32 (2007) 2-18, doi:10.1016/j.pce.2006.04.033
- Delay, J., Forbes, P.-L., Roman J., (2007b), *The Meuse Haute Marne underground research laboratory: seven years of scientific investigations*, Lille
- Piguet J.P., (2001), *French Underground Research Laboratory – Construction and experimental programme, ICEM’01 – Brugge Belgium*.
- Souley M., Armand G., Su K., Wileveau Y., (2007). “Modelling of the hydromechanical response of a shaft sinking in a deep claystone”, tenth International Symposium on Numerical Models in Geomechanics NUMOG X, 25-27 April 2007, Rhodes, Greece, p. 269-275
- Comsol Multiphysics. 2006 Users manuel.
- Lubliner, J. (1990). *Plasticity Theory*, Macmillan Publishing, New York.
- Malvern L.E. (1969). *Introduction to the Mechanics of a Continuous Medium*. Prentice Hall
- Marsden J.E. and Hughes T.J.R. (1983). *Mathematical Foundations of Elasticity*. Dover Publications.
- Rudnicki J.W. and Rice J.R. (1975). Conditions for localization of deformation in pressure sensitive dilatant material. *J. Mech. Phys. Solids*. 23; 371-494.
- Hill R. (1958). “A general theory of uniqueness and stability in elastic plastic solids”. *J. Mech. Phys. Solids*. 6; 236-249.
- Saad Y. and Schultz M. H. (1986). GMRES: A generalized minimal residual algorithm for solving nonsymmetric linear systems, *SIAM J. Sci. Statist. Comput.*, 7, pp. 856–869.